

Scalable Lattice Sampling using Factorized Generative Models

Ali Faraz¹, Ankur Singha², Dipankar Chakrabarti², Vipul Arora^{1*}

^{1*}Department of Electrical Engineering, IIT Kanpur, 208016, Uttar Pradesh, India.

²Department of Physics, IIT Kanpur, 208016, Uttar Pradesh, India.

Abstract

Boltzmann distributions over lattices are pervasive in Computational Physics. Sampling them becomes increasingly difficult with the increase in the number of dimensions, especially near critical regions, e.g., phase transitions or continuum limits. Conditional generative models are emerging as promising tools for sampling in critical regions. When conditioned on the parameters to be varied, they can be efficaciously extended to critical regions, without the need for retraining. However, current approaches do not scale well to large lattices. We present a novel approach called Parallelizable Block Metropolis-within-Gibbs (PBMG) for generating samples for any local lattice model. It factorizes the joint distribution of lattice into local parametric kernels, thereby allowing efficient sampling of very large lattices. We optimize the model with reverse Kullback-Leibler divergence (RKLD) to avoid the need for ground truth samples. Since the local distributions are simpler, the model is not affected by mode collapse, which generally occurs while training with RKLD. We validate our approach on the XY model and the Scalar ϕ^4 theory. PBMG achieves high acceptance rates and the observable statistics estimated from the samples match the ground truth.

Keywords: Markov Chain Monte Carlo, Metropolis-Hastings, Lattice models, Proposal distribution, Scalable and Efficient Sampling

Lattice models in Physics are mathematical models that contain information in the form of a lattice ϕ characterized by Boltzmann distribution defined with the help of a Hamiltonian $H(\phi)$ or action, $s(\phi)$.

$$p(\phi; \theta) \propto e^{-H(\phi; \theta)} \quad (1)$$

Each lattice site is a random variable that could be binary as in an Ising model, angle as in an XY model or real-valued as in scalar ϕ^4 theory. The statistical properties of these lattices vary with parameters θ , showing drastic changes near certain regions of θ called critical regions. Although these distributions are known only up to a normalizing constant, they can be sampled from using statistical methods such as MCMC (Markov Chain Monte Carlo) [1, 2]. These methods provide convergence guarantees that the samples represent the target distribution $p(\phi; \theta)$, they can be quite inefficient, especially in the critical regions. In the critical regions, the correlation between successive samples of the Markov chain (characterized by the autocorrelation time of the chain) becomes very large. This phenomenon is called critical slowing down [3, 4]. Certain algorithms, such as, Swendsen-Wang [5], Wolff [6], worm [7], loop [8], directed loop [9] and HMC (Hamiltonian Monte Carlo) [10], make global MCMC updates to tackle the problem of critical slowing down. However, these methods do not scale well for large lattices.

Generative machine learning (ML) methods are emerging as promising tools to sample Boltzmann distributions. ML methods, such as Gaussian mixture models (GMM) and normalizing flows (NF), that give exact model probabilities can be used in Metropolis-Hastings (MH) algorithm to propose samples which are accepted or rejected. Such algorithms provide convergence guarantees too. NF-based methods have been used for ϕ^4 , 2D Ising model etc. in statistical physics [11–16] and for general Monte Carlo sampling [17]. Self-learning Monte Carlo [18], [19] and Restricted Boltzmann Machines [20] also aim at efficient sampling of lattices using ML methods.

On the other hand, there are ML approaches that do not give exact model probability, and hence, do not guarantee convergence. These include likelihood-free methods, such as, generative adversarial networks [21–23] and likelihood-based methods, such as, variational autoencoders (VAEs) [24] and Boltzmann generators [25]. These methods produce one-shot samples, as opposed to Markov chains.

To address critical slowing down, some ML methods [11] train the generative model for every θ . Since training samples are not available for every θ , Reverse Kullback Leibler divergence (RKL) based learning is used, which is, however, prone to mode collapse (when $p(\phi; \theta)$ is multi-modal but the ML model fails to cover all the modes). Moreover, this approach depends on on-the-fly learning, which could be unstable. As an alternative, the use of conditional generative models is a promising approach [21, 26, 27], where the model learns from samples in non-critical regions and extrapolates or interpolates to critical regions.

However, none of the above ML models scale well with lattice size because they model the entire lattice jointly. We propose factorizing the joint distribution of the lattice and sampling using a Metropolis-within-Gibbs algorithm, with proposals generated by an ML model conditioned on θ . Gibbs algorithm has previously been used with ML models to sample large graphs [28], albeit not for sampling from explicit distribution functions.

We propose Parallelizable Block Metropolis-within-Gibbs (PBMG) algorithm that models a given target distribution by factorizing it into local distributions allowing it to scale well to high-dimensional distributions. The model is used to propose samples for the Metropolis-Hastings (MH) algorithm. We present this method for sampling

from conditional Boltzmann distributions over large lattices. We use conditional generative models, e.g., conditional Gaussian mixture models (GMM) and conditional normalizing flows, to efficiently sample in critical regions. The conditional generative models are generally trained from given samples. However, since generating ground truth samples for large lattices is very difficult, we use RKLD-based training. The problem of mode collapse is avoided in PBMG because the local distributions are much simpler as compared to the joint distributions.

To validate the proposed approach, we apply it to 2-D lattices, namely, the XY model from statistical Physics and the scalar ϕ^4 model from lattice field theory. These two models are described in detail in the Appendix. In the XY model, each lattice site is a spin values (angle) that is locally dependent on immediate neighbors. The lattice distribution is conditioned on temperature T and exhibits phase transition with respect to T , where the magnetic susceptibility diverges. We apply PBMG with conditional rational quadratic spline (RQS) flows for XY lattices. In the scalar ϕ^4 theory, each lattice site is a real number locally dependent on immediate neighbors. The lattice distribution is conditioned on parameters λ and m^2 . We study phase transition with respect to λ , where susceptibility diverges. We apply PBMG with conditional GMMs, conditioned on λ and m^2 , for ϕ^4 theory.

The contributions of this work are multifaceted:

- The introduction of the PBMG algorithm, offering a robust and efficient means to sample Boltzmann distributions over lattices.
- The pioneering factorization of the joint distribution into local components, laying the foundation for scalable sampling in high-dimensional lattice systems.
- The strategic utilization of RKLD optimization to alleviate the need for ground truth samples while mitigating the risk of mode collapse.

1 Parallelizable Block Metropolis-within-Gibbs (PBMG)

Consider an N -dimensional probability distribution $p(\phi_1, \phi_2, \dots, \phi_N)$. For a lattice, N is the number of lattice sites and ϕ_i is the random variable (field, dipole, etc.) at site i . We partition these sites into G partitions such that the distribution of a site i in a partition g , conditioned on all sites $j \notin g$, is independent of all sites $i' \in g \setminus i$.

For implementing MCMC in general state-spaces, one requires to construct a Markov chain transition kernel $p(\phi_i | \phi_{j \neq i})$ that keeps the target distribution $p(\phi_1, \phi_2, \dots, \phi_N)$ invariant, and is ergodic for this distribution. Such kernels can also be combined via composition. Keeping this in mind, let K_i be a transition kernel that updates the site $i \in g$, keeping all other sites of the lattice the same. Then the combined kernel that changes all the sites in the partition g is

$$K_g = \prod_{i \in g} K_i \quad (2)$$

and the overall kernel for updating all the sites in a lattice is

$$K = \prod_g K_g. \quad (3)$$

Here, \prod is the iterative composition function. Such a composition is commonplace in deterministic scan Gibbs samplers. The advantage of partitioning is that all the sites in the same partition can be sampled simultaneously, thereby making the process faster. The term “**Parallelizable Block**” in our algorithm’s nomenclature originates from this inherent capacity to facilitate parallel sampling. Moreover, each kernel K_i need not be conditioned on all the sites outside the partition g , but only a small number of sites in a local neighbourhood of the site i .

Every site-kernel K_i for each $i \in g$ and for every partition g is a Metropolis-within-Gibbs kernel, which means that each site-kernel K_i is a Gibbs kernel with a Metropolis-Hastings accept-reject step. Metropolis-within-Gibbs algorithms, also known as conditional Metropolis-Hastings, are well studied in MCMC [29].

Now, let ϕ_{-i} denote the set of random variables at all the lattice sites excluding the one corresponding to the lattice site i and ψ denote given lattice parameters (e.g., temperature, coupling parameters). Let us define $q(\phi_i^{(t)}; \phi_{-i}, \psi, \theta)$ as the parametric proposal distribution, parameterized by θ . Then, the acceptance probability α_{K_i} for any site-kernel $K_i \forall i \in g$ is

$$\alpha_{K_i} = \frac{p(\phi_i^{(t+1)} | \phi_{-i}, \psi)}{p(\phi_i^{(t)} | \phi_{-i}, \psi)} \cdot \frac{q(\phi_i^{(t)} | \phi_i^{(t+1)}, \phi_{-i}, \psi; \theta)}{q(\phi_i^{(t+1)} | \phi_i^{(t)}, \phi_{-i}, \psi; \theta)} \quad (4)$$

We note that if we design a proposal such that,

$$q(\phi_i^{(t+1)} | \phi_i^{(t)}, \phi_{-i}, \psi; \theta) = q(\phi_i^{(t+1)} | \phi_{-i}, \psi; \theta) \quad (5)$$

i.e., a proposal such that the sampling of the corresponding component is independent of the previous value of the component then the proposal would become an independent proposal (w.r.t. a component). In such a case, the acceptance rate is a direct measure of the performance of the proposal. But it is important to note here that, since, the proposal is an independent proposal w.r.t. a component and not a completely independent proposal, a high acceptance rate cannot guarantee that the integrated autocorrelation time for the observables will be low. This is because the calculation of the integrated autocorrelation time over here involves all the lattice points and not just a single component. Nevertheless, a high acceptance rate would ensure that consecutive samples are very much different from each other which would indirectly lower the autocorrelation within the chain.

This reduces our goal to achieve the maximum acceptance rate possible i.e., an acceptance rate equal to 1. An acceptance rate of 1 will be achieved when $q(\phi_i^{(t+1)} | \phi_{-i}, \psi; \theta)$ is exactly the same as $p(\phi_i^{(t+1)} | \phi_{-i}, \psi)$ and $q(\phi_i^{(t)} | \phi_{-i}, \psi; \theta)$ is exactly the same as $p(\phi_i^{(t)} | \phi_{-i}, \psi)$. This, essentially, reduces our goal to design(or learn) a proposal that could sample from the true conditional distribution as closely as

possible. In order to achieve the above goal, we use methods like Normalizing Flows and Gaussian Mixture Models in probabilistic machine learning. To decide which method to use, we need to first analyze the true conditional distribution for a single component in the two PDFs. In the next two sections, we apply the PBMG method to the XY model and the Scalar ϕ^4 theory. In each section, we first analyze the true conditional distribution for a single component in the corresponding PDF. Subsequently, we discuss the structure of the corresponding proposal distribution, the details of the training procedure and also the inference procedure.

2 Application to XY Model

2.1 Target distribution

The Hamiltonian for the XY model is

$$H(\boldsymbol{\phi}) = -\frac{1}{2} \sum_{\langle i,j \rangle} [\cos(\phi_{i,j} - \phi_{i+1,j}) + \cos(\phi_{i,j} - \phi_{i,j+1}) + \cos(\phi_{i,j} - \phi_{i-1,j}) + \cos(\phi_{i,j} - \phi_{i,j-1})] \quad (6)$$

Here, $\phi_{i,j}$ is the angular random variable with range $[0, 2\pi)$ at the lattice site with coordinates (i, j) . Here, we have used periodic boundary conditions for the lattice. The lattice distribution at a given temperature $T \in \mathbb{R}$ is

$$p(\boldsymbol{\phi}; T) \propto e^{-\frac{H(\boldsymbol{\phi})}{T}} \quad (7)$$

The local Hamiltonian for the (i, j) th component $\phi_{i,j}$ of the lattice vector $\boldsymbol{\phi}$ is

$$H(\phi_{i,j}) = -[\cos(\phi_{i,j} - \phi_{i+1,j}) + \cos(\phi_{i,j} - \phi_{i,j+1}) + \cos(\phi_{i,j} - \phi_{i-1,j}) + \cos(\phi_{i,j} - \phi_{i,j-1})] \quad (8)$$

We see that the Hamiltonian of the (i, j) th component depends only on the components of the four nearest neighbours denoted by $n(i, j) = \{(i+1, j), (i, j+1), (i-1, j), (i, j-1)\}$. Therefore the conditional distribution of $\phi_{i,j}$ given the four nearest neighbour components and temperature is

$$p(\phi_{i,j} | \{\phi_{l,m} : (l, m) \in n(i, j)\}, T) = p(\phi_{i,j} | \mathbf{v}_{i,j}) \propto e^{-\frac{H(\phi_{i,j})}{T}} \quad (9)$$

The above conditional distribution is our target distribution. Here, $\mathbf{v}_{i,j} = (\phi_{i+1,j}, \phi_{i,j+1}, \phi_{i-1,j}, \phi_{i,j-1}, T)$ is the 5x1 condition vector corresponding to the site (i, j) which consists of the four nearest neighbour components and the temperature. For this model, we have divided the lattice into two partitions g_0 and g_1 .

$$g_k = \{(i, j) : (i+j) \% 2 = k\}; k = 0, 1 \quad (10)$$

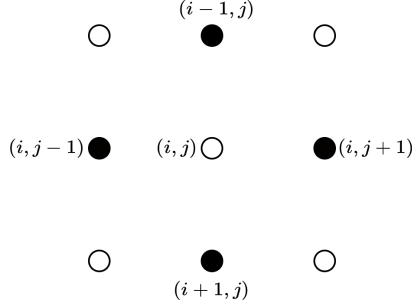


Fig. 1: Partitioning used for a lattice in the XY model. Here, the color white represents partition-1 and the color black represents partition-2.

2.2 Modeling the Proposal distribution

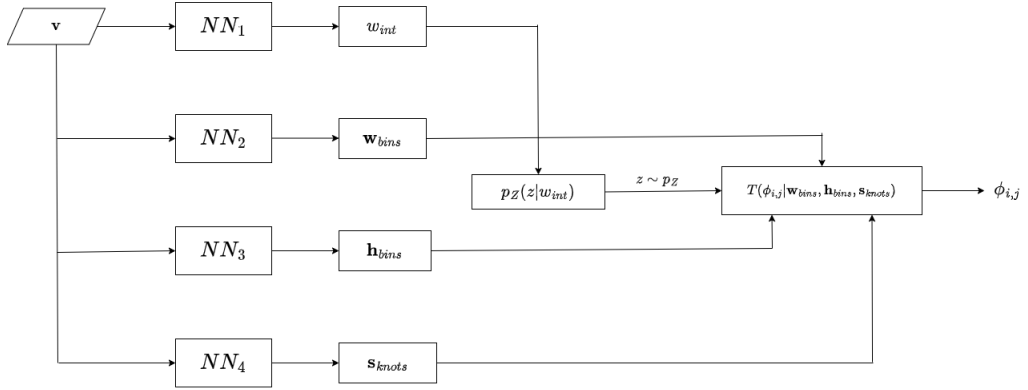


Fig. 2: Proposal distribution for the XY model

We use Normalizing Flows to model the proposal distribution $q(\phi_{i,j} | \mathbf{v}_{i,j}; \boldsymbol{\theta})$. $p_Z(z | \mathbf{v}_{i,j}; \boldsymbol{\theta}_B)$ is the base distribution and $T(z; \boldsymbol{\theta}_R)$ is the invertible transformation used in the Normalizing Flow. Here, $\boldsymbol{\theta} = \{\boldsymbol{\theta}_B, \boldsymbol{\theta}_R\}$. Using the change of variables formula,

$$q(\phi_{i,j} | \mathbf{v}_{i,j}; \boldsymbol{\theta}) = p_Z \left(T^{-1}(\phi_{i,j}; \boldsymbol{\theta}_R) | \mathbf{v}_{i,j}; \boldsymbol{\theta}_B \right) \left| \det \left(\frac{\partial T^{-1}(\phi_{i,j}; \boldsymbol{\theta}_R)}{\partial \phi_{i,j}} \right) \right| \quad (11)$$

We use Rational Quadratic Splines (RQS) as the transform T . An RQS flow is used to map a fixed interval onto another fixed interval. The intervals are partitioned into K bins where each bin is characterized by a rational-quadratic function that increases monotonically. Furthermore, these functions are characterized by $K + 1$ coordinates (referred to as knots) representing boundary values, $K - 1$ derivative values \mathbf{s}_{knots} at

internal knots and the widths \mathbf{w}_{bins} and the heights \mathbf{h}_{bins} of the K bins. For details on RQS flow, one can refer to [30]. The coefficients governing the RQS transformation’s behaviour are adaptable and learned through neural networks. The base distribution is chosen to be uniform, and the interval of the uniform distribution w_{int} is also learnable. We use four different neural networks to learn these parameters, as shown in figure 2.

The parameters of the RQS flow are obtained from the three neural networks NN_2, NN_3, NN_4 , and the interval width of the base distribution is obtained from NN_1 . In eq. 11, the combined set of parameters of NN_2, NN_3 and NN_4 is denoted as $\boldsymbol{\theta}_R$ and the parameters of NN_1 is denoted as $\boldsymbol{\theta}_B$. The condition vector that is input to all the neural networks is \mathbf{v} . The outputs of NN_1 and NN_4 are passed through a Softplus activation function to give the interval width of the base distribution and the $K - 1$ slopes at the intermediate knots, respectively. The outputs of NN_2 and NN_3 are passed through a w_{int} -scaled Softmax activation and a 2π -scaled Softmax activation function to give the widths and the heights of the K bins respectively. We have taken K to be 8.

The architecture of each of the four neural networks is the same except for the output dimension, which is dependent on the output parameter. Each neural network consists of 200 neurons in each hidden layer and three such layers are used. We also use a dropout of 0.3 and a ReLU activation function at each layer except the final one.

2.3 Training and Inference Procedure

The loss function used in the training procedure is the expected value of the KL divergence between the proposal $q(\phi_{i,j}|\mathbf{v}_{i,j};\boldsymbol{\theta})$ and the target $p(\phi_{i,j}|\mathbf{v}_{i,j})$ i.e., the true conditional distribution over all possible values of the condition vector $\mathbf{v}_{i,j}$. The first four components of $\mathbf{v}_{i,j}$ lie in the interval $[0, 2\pi]$ and the last component $T \in [0.05, 2.05]$. We will, therefore, sample $\mathbf{v}_{i,j}$ from $f(\mathbf{v}_{i,j}) = \text{Unif}([0, 2\pi]^4 \times [0.05, 2.05])$ to calculate the expectation.

$$\mathcal{L} = \mathbb{E}_{\mathbf{v}_{i,j} \sim f(\mathbf{v}_{i,j})} \left[\mathbb{E}_{z \sim p_Z(z|\mathbf{v}_{i,j};\boldsymbol{\theta}_B)} [\log q(\phi_{i,j}|\mathbf{v}_{i,j};\boldsymbol{\theta}) - \log p(\phi_{i,j}|\mathbf{v}_{i,j})] \right] \quad (12)$$

$$= \mathbb{E}_{\mathbf{v}_{i,j} \sim f(\mathbf{v}_{i,j})} \left[\mathbb{E}_{z \sim p_Z(z|\mathbf{v}_{i,j};\boldsymbol{\theta}_B)} [\log p_Z(z|\mathbf{v}_{i,j};\boldsymbol{\theta}_B) + \log |\det J_T(z|\mathbf{v}_{i,j};\boldsymbol{\theta}_R)|^{-1} - \log p(T(z;\boldsymbol{\theta}_R)|\mathbf{v}_{i,j})] \right] \quad (13)$$

The Monte Carlo approximation can be used to estimate the above expectation as follows

$$\mathcal{L} \approx \frac{1}{n} \cdot \frac{1}{N} \sum_{r=1}^n \sum_{k=1}^N [\log p_Z(z_k|(\mathbf{v}_{i,j})_r; \boldsymbol{\theta}_B) + \log |\det J_T(z_k|(\mathbf{v}_{i,j})_r; \boldsymbol{\theta}_R)|^{-1} - \log p(T(z_k; \boldsymbol{\theta}_R)|(\mathbf{v}_{i,j})_r)] \quad (14)$$

The procedure for MCMC sampling using PBMG-XY is briefed in the algorithm given below. Here, $\mathbf{V}_g = [\mathbf{v}_{i,j}]_{(i,j) \in g}$.

Algorithm 1: MCMC sampling procedure using PBMG-XY

Initialize: ϕ as $\phi^{(0)}$
for $t = 0$ to $Num - 1$ **do**
 Calculate \mathbf{V}_{g_0} at timestep t
 Condition K_{g_0} on \mathbf{V}_{g_0} and obtain from it $\phi_{i,j}^{(t+1)} \forall (i,j) \in g_0$
 Calculate \mathbf{V}_{g_1} at timestep t
 Condition K_{g_1} on \mathbf{V}_{g_1} and obtain from it $\phi_{i,j}^{(t+1)} \forall (i,j) \in g_1$
end
Return: $\phi^{(0)}, \phi^{(1)}, \dots, \phi^{(t)}$

3 Application to ϕ^4 Theory

The lattice ϕ^4 theory on a 2D lattice has undergone extensive investigation in both statistical mechanics and quantum field theory due to its intricate phase structure and critical behaviour. It demonstrates second-order phase transitions, characterized by alterations in system properties like magnetization or correlation length with varying coupling parameters. For a thorough comprehension of the lattice ϕ^4 model, one can refer to the works [31–33]. In the following section, we will discuss the proposed ML-based sampling approach for the lattice ϕ^4 theory.

3.1 Target Distribution

The Euclidean action for scalar ϕ^4 theory in 2D can be written as,

$$S(\phi, \lambda, m^2) = \sum_{i,j} \left(m^2 + 4 \right) \phi_{i,j}^2 - \phi_{i,j} [\phi_{i+1,j} + \phi_{i,j+1} + \phi_{i-1,j} + \phi_{i,j-1}] + \lambda \phi_{i,j}^4 \quad (15)$$

where (i, j) represents the indices of a lattice site and $\phi_{i,j}$ is a real-valued random variable defined for every lattice site.

The lattice distribution is given by the Boltzmann distribution law,

$$p(\phi | \lambda, m^2) \propto e^{-S(\phi, \lambda, m^2)} \quad (16)$$

The local action for lattice site (i, j) can be written as

$$S_{loc}(\phi_{i,j}, \lambda, m^2, \{\phi_{l,m} : (l, m) \in n(i, j)\}) = S_{loc}(\phi_{i,j}, \lambda, m^2, \kappa_{i,j}) \quad (17)$$

$$= \left(m^2 + 4 \right) \phi_{i,j} + \lambda \phi_{i,j}^4 - 2\phi_{i,j} \kappa_{i,j} \quad (18)$$

where $\kappa_{i,j} = \phi_{i+1,j} + \phi_{i,j+1} + \phi_{i-1,j} + \phi_{i,j-1}$.

We see that the local action for a lattice site depends on its four nearest neighbours i.e. the fields at each lattice site only interact with its nearby lattice points. Therefore,

the conditional distribution of the lattice site (i, j) can be written as

$$p(\phi_{i,j}|\lambda, m^2 + 4, \kappa_{i,j}) = p(\phi_{i,j}|\mathbf{v}_{i,j}) \propto e^{-S_{loc}(\phi_{i,j}, \mathbf{v}_{i,j})} \quad (19)$$

where, $\mathbf{v}_{i,j} = (\lambda, m^2 + 4, \kappa_{i,j})$ is the condition vector for the distribution. Eq. 19 represents the target distribution which we model using the proposed method. For ϕ^4 theory as well, we have divided the lattice into the same two partitions g_0 and g_1 , where

$$g_k = \{(i, j) : (i + j) \% 2 = k\}, k = 0, 1 \quad (20)$$

3.2 Modeling the Proposal Distribution: PBMG- ϕ^4

We construct the proposal distribution for the scalar ϕ^4 theory by using a Gaussian Mixture Model with six Gaussian components. The proposal distribution parameterized by $\boldsymbol{\theta}$, can be written as

$$q(\phi_{i,j}|\mathbf{v}_{i,j}; \boldsymbol{\theta}) = \sum_{k=1}^6 \pi_k(\mathbf{v}_{i,j}) \mathcal{N}(\phi_{i,j}|\mu_k(\mathbf{v}_{i,j}), \sigma_k(\mathbf{v}_{i,j})) \quad (21)$$

where μ_k, σ_k, π_k are the mean, standard deviation and mixing coefficients of the k^{th} Gaussian distribution. These parameters are a function of the condition vector $\mathbf{v}_{i,j} = (\lambda, m^2 + 4, \{\phi_{l,m} : (l, m) \in n(i, j)\})$. This function could be a neural network whose parameters can be optimized using a suitable loss function. The input to the k^{th} neural network is the condition vector $\mathbf{v}_{i,j}$, and the outputs are the parameters $(\mu_k, \log(\sigma_k), \pi_k)$.

The architectures of all six neural networks are the same, with the only difference lying in the initialization of the network parameters. In each neural network, we use three dense layers with 150 neurons in each layer, and a ReLU activation function at each layer except the final one. The neurons in the final layer use linear activation. The value of $\log(\sigma_k) > 1$ is clipped to 1. Since $\sum_k \pi_k = 1$, the networks output logit values that are converted to π_k by applying softmax.

3.3 Training and Inference Procedure

The training procedure of PBMG- ϕ^4 is similar to that of PBMG-XY. The loss function used in the training procedure is the expected value of the KL divergence between the proposal $q(\phi_{i,j}|\mathbf{v}_{i,j}; \boldsymbol{\theta})$ and the target $p(\phi_{i,j}|\mathbf{v}_{i,j})$ i.e., the true conditional distribution over all possible values of the condition vector $\mathbf{v}_{i,j}$ along with an L_2 regularization term. The effect of the regularization term is that the mixing coefficients remain close to each other and this in turn stabilizes the training. We train our model for the following range of the parameters: $\lambda \in [2.5, 15]$, $m^2 \in [-8, 0]$ and $\kappa_{i,j} \in [0, 3]$. We will, therefore, sample $\mathbf{v}_{i,j}$ from $f(\mathbf{v}_{i,j}) = \text{Unif}([2.5, 15] \times [-4, 4] \times [0, 3])$ to calculate the expectation. Here, $\boldsymbol{\pi}(\mathbf{v}_{i,j}) = [\pi_k(\mathbf{v}_{i,j})]_{k=1}^6$ and $\|\cdot\|$ represents the L_2 norm.

$$\mathcal{L} = \mathbb{E}_{\mathbf{v}_{i,j} \sim f(\mathbf{v}_{i,j})} \left[\mathbb{E}_{\phi_{i,j} \sim q(\phi_{i,j}|\mathbf{v}_{i,j}; \boldsymbol{\theta})} \left[\log \frac{q(\phi_{i,j}|\mathbf{v}_{i,j}; \boldsymbol{\theta})}{p(\phi_{i,j}|\mathbf{v}_{i,j})} \right] + \|\boldsymbol{\pi}(\mathbf{v}_{i,j})\| \right] \quad (22)$$

And the Monte Carlo approximation to the above expression is

$$\mathcal{L} \approx \frac{1}{n} \sum_{r=1}^n \left[\frac{1}{N} \sum_{k=1}^N [\log q((\phi_{i,j})_k | (\mathbf{v}_{i,j})_r; \boldsymbol{\theta}) - \log p((\phi_{i,j})_k | (\mathbf{v}_{i,j})_r)] + \|\boldsymbol{\pi}((\mathbf{v}_{i,j})_r)\| \right] \quad (23)$$

The procedure for MCMC sampling using PBMG- ϕ^4 is exactly the same as that of PBMG-XY given in Algorithm-1.

4 Experiments for PBMG-XY

In this section, we evaluate the PBMG-XY model against the ground truth which we generate using plain-MCMC. We carry out the experiments for five lattice sizes i.e., for $L = 8, 16, 32, 64, 128$. For each lattice size, we simulate for 32 temperatures, evenly spaced within the range $[0.05, 2.05]$. We use the observables Mean Energy, Mean Magnetization and Mean Vorticity and the metrics Earth Mover Distance (EMD) and Percentage Overlap (%OL) in our experiments to compare the performance of our model with that of the ground truth. A brief explanation regarding them is provided below. Further details can be found in Appendix A.2 and Appendix C. Here, consider a set of N samples of $L \times L$ lattices $\{\phi_1, \phi_2, \dots, \phi_N\}$.

Mean Energy: The Hamiltonian of a lattice sample divided by the number of lattice points is the mean energy $E(\phi_i)$ of that lattice sample ϕ_i . The observable mean energy is defined as the average mean energy per lattice sample.

$$\langle E \rangle = \frac{1}{N} \sum_{i=1}^N E(\phi_i) = \frac{1}{N} \cdot \frac{1}{L^2} \sum_{i=1}^N H(\phi_i) \quad (24)$$

Mean Magnetization: The magnetization of a lattice sample is

$$M(\phi) = \left| \frac{1}{L^2} \left(\sum_{\langle i,j \rangle} \cos(\phi_{i,j}) \right) \hat{\mathbf{x}} + \frac{1}{L^2} \left(\sum_{\langle i,j \rangle} \sin(\phi_{i,j}) \right) \hat{\mathbf{y}} \right| \quad (25)$$

and the mean magnetization of a set of lattice samples is,

$$\langle M \rangle = \frac{1}{N} \sum_{i=1}^N M(\phi_i) \quad (26)$$

Mean Vorticity: The average vorticity across all the lattice samples is defined as the mean vorticity. Here, $V_o(\phi_i)$ is the Vorticity of the lattice sample ϕ_i . For details refer to Appendix A.2.

$$\langle V_o \rangle = \frac{1}{N} \sum_{i=1}^N V_o(\phi_i) \quad (27)$$

Earth Mover Distance: EMD (aka Wasserstein Metric) is a distance metric and denotes, in a sense, the distance between any two probability distributions. The

mathematical definition of EMD is given below. Here, H_M and H_G are the normalized histograms generated out of the ground truth samples and the samples from PBMG-XY respectively.

$$\text{EMD}(H_M, H_G) = \sum_{x=-\infty}^{+\infty} \left| \sum_{t=-\infty}^x (H_M(t) - H_G(t)) \right| \quad (28)$$

Percentage Overlap (%OL): %OL is a similarity metric and, as the name suggests, gives the overlap (in percentage) between the two normalized histograms H_M and H_G . The formula for %OL is as follows.

$$\%OL(H_M, H_G) = \sum_i \min(H_M(i), H_G(i)) \quad (29)$$

The plain-MCMC algorithm is used for the generation of ground truth. We generate 10,000 samples for each temperature by thinning, selecting every k th sample. k varies for each lattice size but remains constant for all temperatures for that size (shown in table 1). Burn-in is unnecessary as we initiate the Markov chain from the highest probability point with all spins at zero.

L	8	16	32	64	128
Value of k	120	400	1300	5000	20000

Table 1: Value of k for thinning for each lattice size

In our PBMG-XY simulations, different ensemble sizes were generated across 32 temperatures for each lattice size. These ensemble sizes were determined based on anticipated auto-correlation levels. Higher auto-correlation necessitated more samples to ensure accurate estimation of observables. Appendix D provides the details of the ensemble size generated for each temperature and lattice size.

4.1 Results and Observations

We estimate the mean magnetization and the mean vorticity on a lattice of size $L = 16$ as shown in figure 3. Similarly, we estimate the mean energy and the mean vorticity on a larger lattice of size $L = 128$ as shown in figure 4. The remaining figures for the observables estimated on other lattice sizes can be found in Appendix E.

We observe that the graphs of the observables are matching to a great extent. Only in a few regions and for a few lattice sizes and observables, the discrepancy is considerable and this is because the length of the Markov chain that is generated from the model in those areas is short according to the auto-correlation that exists within the samples. The factor that restricts us from taking even longer chains is the simulation time. The acceptance rate for PBMG-XY varies considerably but lay mostly in the range of 80-95%. This variation could be due to the below-par learning of

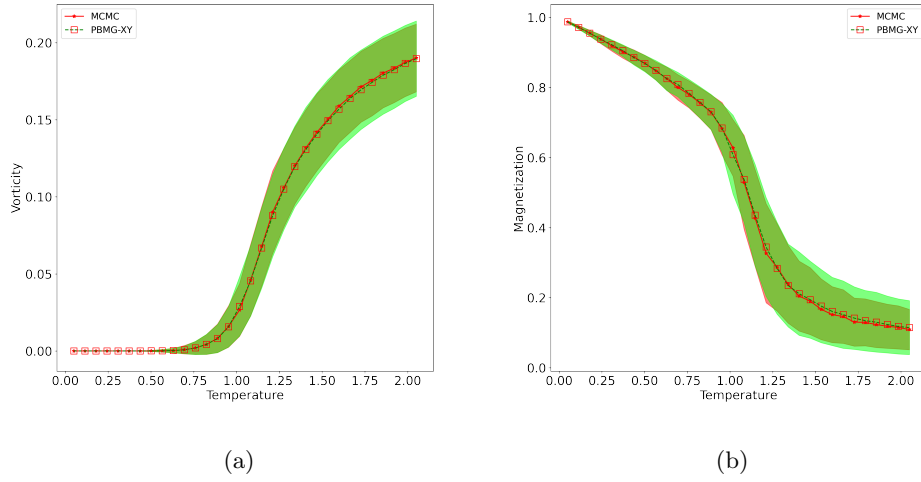


Fig. 3: a) Mean Vorticity and b) Mean Energy plots superimposed for $L=16$.

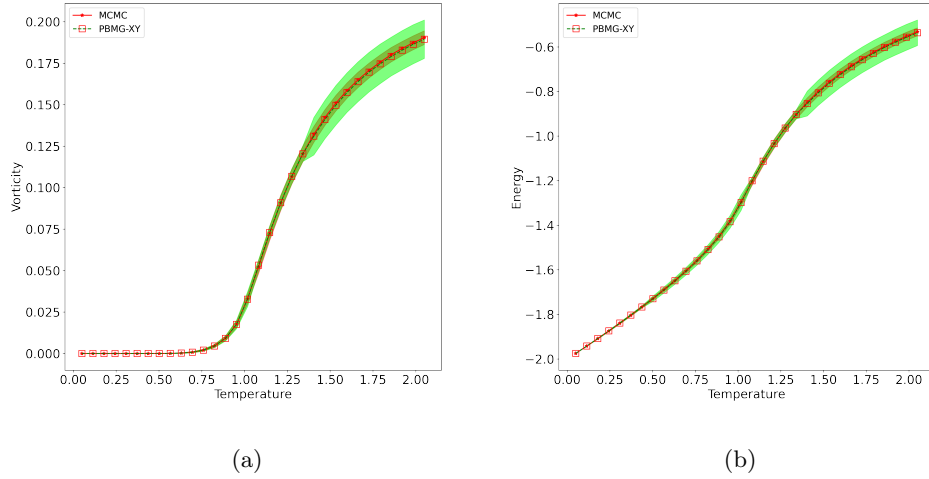


Fig. 4: a) Mean Energy and b) Mean Vorticity plots superimposed for $L=128$

the target conditional distributions for a few sets of conditions. We speculate that the below-average learning results could be attributed to employing a training approach that was not conducive to achieving optimal learning outcomes in spline flows.

Table 2 shows the comparison of EMD and %OL for the observable mean energy. The remaining two tables for the observables mean magnetization and mean vorticity

L	EMD		% OL	
	Mean	Std	Mean	Std
8	0.009	0.012	68.138	13.638
16	0.006	0.007	69.849	13.682
32	0.003	0.002	75.619	11.469
64	0.002	0.002	75.553	10.799
128	0.001	0.001	75.819	9.260

Table 2: Metrics for Mean Energy

are given in Appendix E. In table 2, we observe that the EMD between the ground truth and the model is quite low and the %OL between the two is quite high.

5 Experiments and Results for PBMG- ϕ^4

In this section, we evaluate the PBMG- ϕ^4 model against the ground truth which we generate using Hamiltonian Monte Carlo simulation. For the ϕ^4 theory, we conduct two kinds of experiments. One is on the computation of the lattice observables, and the other is on the computation of integrated auto-correlation time.

5.1 Experiment on Observables

We compute various observables on the lattice ensembles such as the mean ϕ^2 value, two-point susceptibility, and two-point correlation function from both HMC and PBMG- ϕ^4

One of the key observables estimated in lattice ϕ^4 theory is the ‘‘correlation function’’ or ‘‘two-point function’’. This observable measures the correlation or interaction between field operators at different lattice sites across space. The correlation function can be written as

$$G_c(i, j) = \frac{1}{V} \sum_{l, m} [\langle \phi_{l, m} \phi_{i+l, j+m} \rangle - \langle \phi_{l, m} \rangle \langle \phi_{i+l, j+m} \rangle].$$

and the zero momentum correlation function is defined as

$$C(t) = \sum_i G_c(i, t),$$

where $t = j$ is the time axis. The pole mass and two-point susceptibility can be derived from $C(t)$ and $G(i, j)$,

$$m_p = \log \left[\frac{C(t+1)}{C(t)} \right]; \quad \chi = \sum_i G(i, j).$$

The mean magnetization can be estimated as

$$\langle |\tilde{\phi}| \rangle : \tilde{\phi} = \frac{1}{V} \sum_{i,j} \phi_{i,j}.$$

The experiment on the observables was carried out for five lattice sizes, i.e., $L = 8, 16, 24, 32, 48, 64,$ and 128 . The parameter m^2 is fixed at -4 for all the ensembles. While preparing the ground truth, the numbers of MD steps N and step-size ϵ in HMC are adjusted so that the acceptance rate and the auto-correlation time remain almost constant for all the lattice sizes in the experiment. The acceptance rate is between 70% to 85%, and the auto-correlation time is around 5 for all the lattice sizes. For every lattice size, 50K samples are generated. We consider every fifth lattice sample for the calculation of observables i.e. 10K samples are considered for the final estimation of each observable.

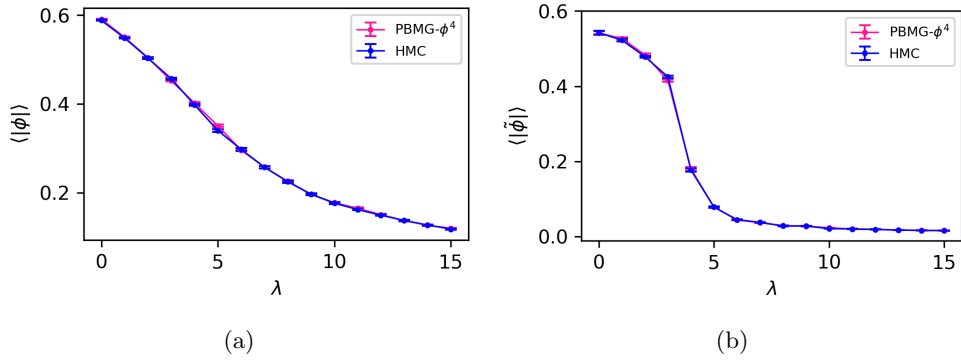


Fig. 5: a) Two-point susceptibility compared between HMC and PBMG- ϕ^4 for $L=8$ and b) Absolute mean ϕ value for $L=64$

In the PBMG- ϕ^4 model, different thinning and ensemble sizes are used for different lattice sizes. For $L = 8, 16,$ and 32 , we generate 250K samples, and every 25th sample is used for measurement, bringing down the number of samples to 10K. For $L = 64$ and 128 , 100K samples are generated, and every 10th sample is used for measurement.

While estimating uncertainties, we use bootstrap error analysis with a bin size of 100 for all the observables. In Figure 5a, we calculate two-point susceptibility across the parameter λ keeping $m^2 = -4$ for $L = 8$. Similarly, in Figure 5b, we compute the absolute mean ϕ for larger lattice size i.e. $L = 64$. We can infer a second-order phase transition behaviour which is characteristic of lattice ϕ^4 theory in 2D. We also calculate the zero momentum correlation function for $L = 8$ and 32 for $\lambda = 5.4$ and $m^2 = -4$. Here, we observe the expected behaviour i.e., we observe that the correlation between the sites decreases as we move to the centre of the lattice from the origin, and it is symmetric due to the periodicity in the lattice. We also compute pole mass from both HMC and PBMG- ϕ^4 model by varying λ and lattice size L as shown in Table 3. We

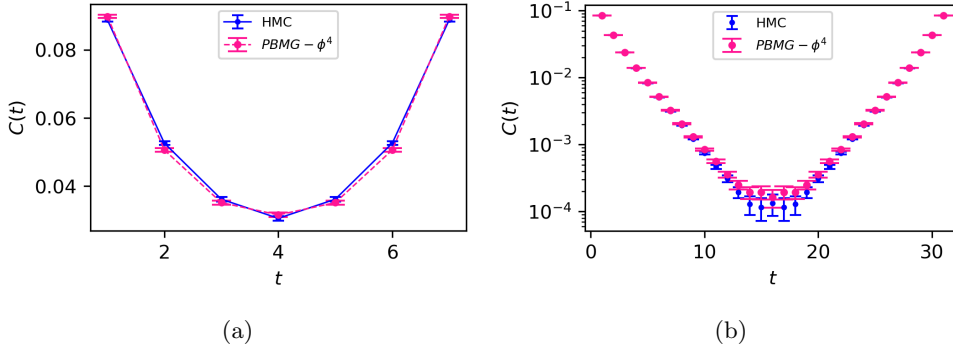


Fig. 6: Two point Correlation function compared between HMC and PBMG- ϕ^4 for lattice size a) 8×8 and b) 32×32

Ensemble	S1	S2	S3	S4	S5
m^2	-4	-4	-4	-4	-4
L	16	24	32	48	64
λ	8	6.3	5.6	5.0	4.8
$m_p L$	12.80(2)	12.79(4)	12.82(5)	12.87(8)	12.81(3)

Table 3: Set of ensemble studied where the parameter λ and L are varied while keeping $m_p L$ fixed at ≈ 12.8 .

tune the λ and L such that the pole mass remains constant, and at the same time, we move towards the critical region. The pole mass for ensemble $S3$ is shown in Figure 7 which we compute from both HMC and PBMG- ϕ^4 generated samples.

We see a significant agreement between all the observables which we calculate from HMC and PBMG- ϕ^4 model within statistical uncertainty.

5.2 Experiment on Autocorrelation

The integrated auto-correlation time measures the total correlation length in a Markov chain. It roughly quantifies how many configurations, on average, need to be skipped to obtain effectively independent configurations. For an observable A , the integrated auto-correlation time, denoted by τ_{int} , is defined as

$$\tau_{int} = 1 + 2 \sum \frac{C(k)}{C(0)} \quad (30)$$

where the sum runs from $k = 1$ to infinity, and $C(k)$ is the auto-correlation function of the observable A at lag k (the correlation between A at configuration i and A at configuration $i + k$). $C(0)$ is the auto-correlation at zero lag.

We compute the autocorrelation of two-point susceptibility χ . We perform these experiments for $m^2 = -4$ and $\lambda = 5.4$, such that we remain quite close to the critical region of the theory.

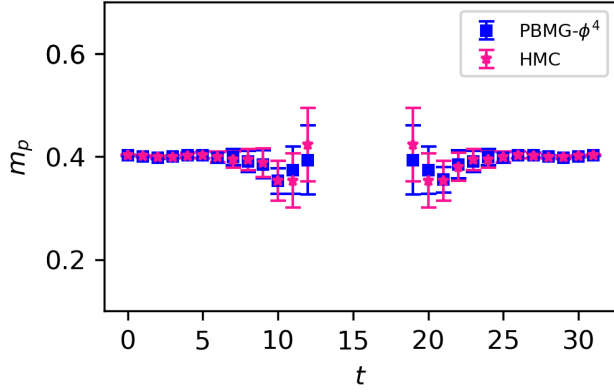


Fig. 7: Effective mass computed for parameter $\lambda = 5.4$ and $L = 32$ from lattice ensemble generated by HMC and PBMG- ϕ^4 model. We ignore points in the middle of time axis due to high noise

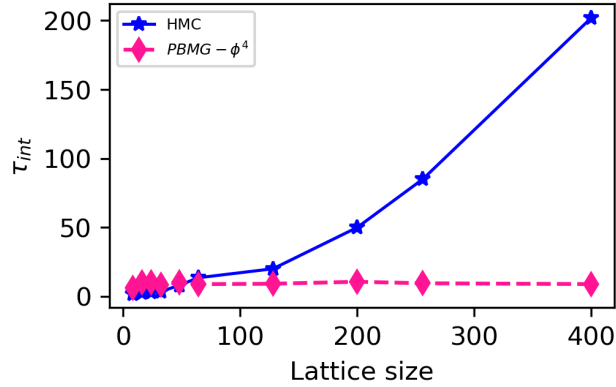


Fig. 8: Integrated autocorrelation time τ of two point susceptibility for lattice ensemble generated from HMC and PBMG- ϕ^4 model

We know that in HMC, the simulation cost rapidly increases as the volume of the lattice increases. Hence, simulation near the critical region becomes difficult where one needs finer lattices with large lattice volumes. This is because auto-correlation shoots up as we move towards the critical region. Therefore to compare the efficiency of our model for simulation in the critical region, we computed integrated auto-correlation time (τ) for different lattice sizes from 8×8 upto 400×400 from both HMC and PBMG- ϕ^4 method. For each lattice volume, 10k samples are generated from both HMC and PBMG- ϕ^4 model. For HMC, we fixed the parameter MD step size to 0.01 and the number of MD steps to 20 so that for the smallest lattice, the acceptance rate and auto-correlation are comparable for both methods.

Figure 8 shows how the integrated auto-correlation time(τ) varies as we increase the lattice size in both methods. As we sample for larger lattice sizes, (τ) increases rapidly in the case of HMC. On the other hand, from the PBMG- ϕ^4 model, we see a constant τ as we sample for different lattice sizes. Furthermore, we observe an almost-constant acceptance rate of around 98% from our model PBMG- ϕ^4 irrespective of the lattice size and the parameters for which the simulation is carried out. This is a significant gain in terms of sampling cost while simulating a larger lattice volume.

6 Conclusion and Future Scope

In this study, we have introduced a novel method, Parallelizable Block Metropolis-within-Gibbs (PBMG), designed to address the challenge of efficiently sampling Boltzmann distributions for large lattices. By decomposing the complicated joint distribution into simpler local conditional distributions, our approach leverages the power of generative machine learning, offering a scalable solution that transcends the limitations of traditional sampling methods. Through our experiments on the XY model and the Scalar ϕ^4 theory, we have demonstrated the efficacy of our approach.

The PBMG models are trained using the Reverse KL objective, negating the need for existing simulated data. The trained models can be employed across various lattice sizes, eliminating the need for retraining. The design of the proposal ensures that the acceptance rate remains unaffected by the lattice size under simulation. Furthermore, the models are conditioned on the action parameters enabling us to simulate using them at multiple parameter values. PBMG not only matches the performance of baseline methods for smaller lattices but also outperforms them in terms of simulation cost for larger lattices.

In the context of the XY model, our results exhibit a significant match of observables and commendable values of metrics, providing a solid foundation for the accuracy of our approach. For the Scalar ϕ^4 theory, PBMG showcases even better results with very high and consistent acceptance rates, indicating efficient sampling even near critical regions. The most remarkable observation from our experiments is the constant integrated autocorrelation time across different lattice sizes exhibited by PBMG- ϕ^4 , a clear testament to its efficiency in sampling and capturing physics near the critical region.

While our accomplishments are noteworthy, there remain avenues for enhancement. Further optimization of training procedures, specially tailored for Monotonic RQS flows, could lead to improved acceptance rates and reduced variation in PBMG-XY. Moreover, the successful extension of PBMG to 3D and 4D lattices holds tantalizing prospects for advancing research in this domain.

7 Acknowledgements

We gratefully acknowledge the invaluable assistance provided by Prof. Dootika Vats (Dept. of Mathematics and Statistics, IIT Kanpur), in guiding us through the mathematical intricacies involved in this research.

References

- [1] Metropolis, N., Rosenbluth, A.W., Rosenbluth, M.N., Teller, A.H., Teller, E.: Equation of state calculations by fast computing machines. *The journal of chemical physics* **21**(6), 1087–1092 (1953)
- [2] Hastings, W.K.: *Monte carlo sampling methods using markov chains and their applications* (1970)
- [3] Wolff, U.: Critical slowing down. *Nuclear Physics B - Proceedings Supplements* **17**, 93–102 (1990) [https://doi.org/10.1016/0920-5632\(90\)90224-I](https://doi.org/10.1016/0920-5632(90)90224-I)
- [4] Schaefer, S., Sommer, R., Virotta, F., Collaboration, A., *et al.*: Critical slowing down and error analysis in lattice qcd simulations. *Nuclear Physics B* **845**(1), 93–119 (2011)
- [5] Swendsen, R.H., Wang, J.-S.: Nonuniversal critical dynamics in monte carlo simulations. *Phys. Rev. Lett.* **58**, 86–88 (1987) <https://doi.org/10.1103/PhysRevLett.58.86>
- [6] Wolff, U.: Collective monte carlo updating for spin systems. *Phys. Rev. Lett.* **62**, 361–364 (1989) <https://doi.org/10.1103/PhysRevLett.62.361>
- [7] Prokof'ev, N.V., Svistunov, B.V., Tupitsyn, I.S.: “worm” algorithm in quantum monte carlo simulations. *Physics Letters A* **238**(4), 253–257 (1998) [https://doi.org/10.1016/S0375-9601\(97\)00957-2](https://doi.org/10.1016/S0375-9601(97)00957-2)
- [8] Evertz, H.G., Lana, G., Marcu, M.: Cluster algorithm for vertex models. *Phys. Rev. Lett.* **70**, 875–879 (1993) <https://doi.org/10.1103/PhysRevLett.70.875>
- [9] Syljuåsen, O.F., Sandvik, A.W.: Quantum monte carlo with directed loops. *Phys. Rev. E* **66**, 046701 (2002) <https://doi.org/10.1103/PhysRevE.66.046701>
- [10] Neal, R.M., *et al.*: Mcmc using hamiltonian dynamics. *Handbook of markov chain monte carlo* **2**(11), 2 (2011)
- [11] Albergo, M.S., Kanwar, G., Shanahan, P.E.: Flow-based generative models for markov chain monte carlo in lattice field theory. *Physical Review D* **100**(3), 034515 (2019)
- [12] Albergo, M.S., Kanwar, G., Racanière, S., Rezende, D.J., Urban, J.M., Boyda, D., Cranmer, K., Hackett, D.C., Shanahan, P.E.: Flow-based sampling for fermionic lattice field theories. *Phys. Rev. D* **104**(11), 114507 (2021) <https://doi.org/10.1103/PhysRevD.104.114507> [arXiv:2106.05934](https://arxiv.org/abs/2106.05934) [hep-lat]
- [13] Albergo, M.S., Boyda, D., Cranmer, K., Hackett, D.C., Kanwar, G., Racanière, S., Rezende, D.J., Romero-López, F., Shanahan, P.E., Urban, J.M.: Flow-based sampling in the lattice Schwinger model at criticality. *Phys. Rev. D* **106**(1),

- 014514 (2022) <https://doi.org/10.1103/PhysRevD.106.014514> arXiv:2202.11712 [hep-lat]
- [14] Hackett, D.C., Hsieh, C.-C., Albergo, M.S., Boyda, D., Chen, J.-W., Chen, K.-F., Cranmer, K., Kanwar, G., Shanahan, P.E.: Flow-based sampling for multimodal distributions in lattice field theory. arXiv:2107.00734 (2021) [arXiv:2107.00734](https://arxiv.org/abs/2107.00734) [hep-lat]
- [15] Nicoli, K.A., Nakajima, S., Strodthoff, N., Samek, W., Müller, K.-R., Kessel, P.: Asymptotically unbiased estimation of physical observables with neural samplers. Phys. Rev. E **101**, 023304 (2020) <https://doi.org/10.1103/PhysRevE.101.023304>
- [16] Nicoli, K.A., Anders, C.J., Funcke, L., Hartung, T., Jansen, K., Kessel, P., Nakajima, S., Stornati, P.: Estimation of thermodynamic observables in lattice field theories with deep generative models. Phys. Rev. Lett. **126**, 032001 (2021) <https://doi.org/10.1103/PhysRevLett.126.032001>
- [17] Song, J., Zhao, S., Ermon, S.: A-NICE-MC: Adversarial Training for MCMC. arXiv (2017). <https://doi.org/10.48550/ARXIV.1706.07561> . <https://arxiv.org/abs/1706.07561>
- [18] Liu, J., Qi, Y., Meng, Z.Y., Fu, L.: Self-learning monte carlo method. Phys. Rev. B **95**, 041101 (2017) <https://doi.org/10.1103/PhysRevB.95.041101>
- [19] Chen, C., Xu, X.Y., Liu, J., Batrouni, G., Scalettar, R., Meng, Z.Y.: Symmetry-enforced self-learning monte carlo method applied to the holstein model. Phys. Rev. B **98**, 041102 (2018) <https://doi.org/10.1103/PhysRevB.98.041102>
- [20] Huang, L., Wang, L.: Accelerated monte carlo simulations with restricted boltzmann machines. Physical Review B **95**(3), 035105 (2017)
- [21] Singh, J., Scheurer, M.S., Arora, V.: Conditional generative models for sampling and phase transition indication in spin systems. SciPost Phys. **11**, 043 (2021) <https://doi.org/10.21468/SciPostPhys.11.2.043>
- [22] Singha, A., Chakrabarti, D., Arora, V.: Generative learning for the problem of critical slowing down in lattice Gross-Neveu model. SciPost Phys. Core **5**, 052 (2022) <https://doi.org/10.21468/SciPostPhysCore.5.4.052> arXiv:2111.00574 [hep-lat]
- [23] Pawłowski, J.M., Urban, J.M.: Reducing autocorrelation times in lattice simulations with generative adversarial networks. Machine Learning: Science and Technology **1**(4), 045011 (2020)
- [24] Cristoforetti, M., Jurman, G., Nardelli, A.I., Furlanello, C.: Towards meaningful physics from generative models. arXiv (2017). <https://doi.org/10.48550/ARXIV.1705.09524> . <https://arxiv.org/abs/1705.09524>

- [25] Noé, F., Olsson, S., Köhler, J., Wu, H.: Boltzmann generators: Sampling equilibrium states of many-body systems with deep learning. *Science* **365**(6457), 1147 (2019) <https://doi.org/10.1126/science.aaw1147> <https://www.science.org/doi/pdf/10.1126/science.aaw1147>
- [26] Singha, A., Chakrabarti, D., Arora, V.: Conditional normalizing flow for Markov chain Monte Carlo sampling in the critical region of lattice field theory. *Phys. Rev. D* **107**(1), 014512 (2023) <https://doi.org/10.1103/PhysRevD.107.014512>
- [27] Singha, A., Chakrabarti, D., Arora, V.: Sampling $U(1)$ gauge theory using a re-trainable conditional flow-based model (2023) [arXiv:2306.00581](https://arxiv.org/abs/2306.00581) [hep-lat]
- [28] Wang, T., Wu, Y., Moore, D., Russell, S.J.: Meta-learning mcmc proposals. *Advances in neural information processing systems* **31** (2018)
- [29] Jones, G.L., Roberts, G.O., Rosenthal, J.S.: Convergence of conditional Metropolis-Hastings samplers. *Advances in Applied Probability* **46**(2), 422–445 (2014)
- [30] Durkan, C., Bekasov, A., Murray, I., Papamakarios, G.: Neural spline flows. *Advances in neural information processing systems* **32** (2019)
- [31] De, A.K., Harindranath, A., Maiti, J., Sinha, T.: Investigations in 1 + 1 dimensional lattice ϕ^4 theory. *Phys. Rev. D* **72**, 094503 (2005) <https://doi.org/10.1103/PhysRevD.72.094503>
- [32] De, A.K., Harindranath, A., Maiti, J., Sinha, T.: Topological charge in 1 + 1 dimensional lattice ϕ^4 theory. *Phys. Rev. D* **72**, 094504 (2005) <https://doi.org/10.1103/PhysRevD.72.094504>
- [33] Vierhaus, I.: Simulation of phi 4 theory in the strong coupling expansion beyond the ising limit. Master's thesis, Humboldt-Universität zu Berlin, Mathematisch-Naturwissenschaftliche Fakultät I (2010). <https://doi.org/10.18452/14138>

Appendix A Review of the 2D XY model

A.1 Probabilistic formulation of the 2D XY model

The XY model is one of the simpler lattice models in statistical mechanics. Each lattice site in this model consists of a vector of unit magnitude $\mathbf{s}_{i,j} = (\cos \phi_{i,j}, \sin \phi_{i,j})^T$ where $\phi_{i,j} \in [0, 2\pi)$ and (i, j) denote the exact position of the lattice site. These unit vectors are referred to as spins. A spin $\mathbf{s}_{i,j}$ is characterised by the angle $\phi_{i,j}$. The Hamiltonian of the configuration ϕ is given by,

$$H(\phi) = - \sum_{\langle(i,j),(k,l)\rangle} \mathbf{s}_{i,j} \cdot \mathbf{s}_{k,l} = - \sum_{\langle(i,j),(k,l)\rangle} \cos(\phi_{i,j} - \phi_{k,l}) \quad (\text{A1})$$

where the sum is taken such that the lattice sites (i, j) and (k, l) are neighbors. Each pair of neighbours is counted exactly once. Here, we have considered only those nearest-neighbour interactions which are ferromagnetic in nature i.e., we have assumed $J > 0$. Furthermore, we have taken $J \equiv 1$ i.e., we've taken it as the unit of energy.

Using the Boltzmann distribution formulation, the probability density function for a temperature $T > 0$ is,

$$p(\phi; T) = \frac{1}{Z(T)} \exp\left(-\frac{H(\phi)}{T}\right) \quad (\text{A2})$$

Here, the normalizing constant $Z(T)$ (also known as partition function) is the integral of $\exp\left(-\frac{H(\phi)}{T}\right)$ over all possible configurations. Note that we have set the Boltzmann constant (k_B) to unity over here.

A.2 Observables in the 2D XY model

The macroscopic properties of the XY model at a given temperature that can be measured or observed are referred to as observables. From a probabilistic perspective, these observables are actually expected values of certain lattice functions (by this I mean functions that take in a lattice as input and give some output) over all possible configurations of lattices. Mathematically,

$$\langle f_O \rangle = \int_{\phi} f_O(\phi) p(\phi; T) d\phi \quad (\text{A3})$$

Mean Energy, Mean Magnetization, Mean Vorticity and Magnetic Susceptibility are observables of the XY model. We will see here the expressions of Monte Carlo estimation for the observables Mean Vorticity and Magnetic Susceptibility. Here, $\phi_1, \phi_2, \dots, \phi_N$ are taken as the drawn-out lattice samples. It is important to remember that all of these are calculated for a system at a given temperature T .

Mean Vorticity (V_o) - For calculating this, we first construct a matrix, in each entry of which we enter the sum of the angle differences in anti-clockwise sense across the 3 by 3 square centred at that entry i while keeping each angle difference in the

range of $(-\pi, \pi]$ using a saw function. Once we fill the whole matrix like this, the whole matrix is then divided by 2π and each element is then rounded to the nearest integer. After this, we count the number of entries that are equal to 1. This count is then divided by the total number of entries in the matrix i.e., L^2 because the size of the lattice is $L \times L$. This resulting number is defined as the Vorticity (V_o) of a configuration. The mean vorticity is then calculated by taking the average of these vorticities across all the lattice samples.

$$\langle V_o \rangle = \frac{1}{N} \sum_{i=1}^N V_o(\phi_i) \quad (\text{A4})$$

Magnetic Susceptibility (χ) - The variance of the magnetization across the set of lattice samples is defined as the magnetic susceptibility.

$$\chi = \text{var}(M) = \langle M^2 \rangle - \langle M \rangle^2 = \frac{1}{N} \sum_{i=1}^N M^2(\phi_i) - \left(\frac{1}{N} \sum_{i=1}^N M(\phi_i) \right)^2 \quad (\text{A5})$$

A.3 The BKT transition

‘BKT’ in the BKT transition stands for Berezinskii-Kosterlitz-Thouless. This transition is a characteristic phenomenon of the XY model. It is a phase transition that takes place at the critical temperature T_c due to the unbinding of vortex-antivortex pairs. It is a first-order transition and the magnetic susceptibility (and other parameters of similar order) diverge because of it. This transition is the cause behind the relatively difficult simulation of the XY model as compared to other models with a higher-order parameter that smoothly changes with temperature. Simulation of the XY model in the critical region (i.e. near the critical temperature T_c) is relatively difficult as compared to simulation at lower or higher temperatures. For $J = k$, the critical temperature $T_c \approx 0.9$.

Appendix B Metrics for experiments in the case of PBMG-XY

We discuss here the different metrics that we have used to compare the performance of our model with the ground truth generated using plain-MCMC. These metrics, essentially, indicate the similarity between two histograms or probability distributions and we use these metrics because we want to estimate the similarity between the histogram we generate out of our model and the histogram generated from plain-MCMC.

B.1 Earth Mover Distance

Considering each distribution to be a pile of dirt, EMD is the minimum cost of transforming one pile into the other. A lower value of EMD indicates a higher matching percentage of the two probability distributions. For each lattice size (L) and for

each temperature, we generate a number of lattices from the model and from plain-MCMC(which is taken as the ground truth). We then generate normalized histograms (H_M & H_G) out of these two sets of lattices and then calculate the EMD between these two histograms.

$$\text{EMD}(H_M, H_G) = \sum_{x=-\infty}^{+\infty} \left| \sum_{t=-\infty}^x (H_M(t) - H_G(t)) \right| \quad (\text{B6})$$

B.2 Percentage Overlap

The accuracy of %OL is less than that of EMD because relatively accurate observables may look dissimilar w.r.t this metric i.e., may get a small value of percentage overlap. To calculate %OL we take the minimum of the two histogram values for each index and sum over all indices. In the expression below, i is the bin index corresponding to which the minimum is being calculated.

$$\%OL(H_M, H_G) = \sum_i \min(H_M(i), H_G(i)) \quad (\text{B7})$$

Appendix C Details of simulation from PBMG-XY during experiments

For most temperatures, we have generated 10,000 samples and that's why, in the tables below, we have included only those temperatures for which we have generated more than 10,000 samples.

Temperature	0.05	0.115	0.179	0.244	0.308	0.373	0.437
Number of samples	50000	45000	40000	35000	30000	25000	20000

Table C1: Number of generated samples(other than those with 10,000) for $L = 8$

Temperature	0.05	0.115	0.179	0.244	0.308	0.373
Number of samples	50000	45000	40000	35000	30000	25000
Temperature	0.437	1.082	1.147	1.211	1.276	1.340
Number of samples	20000	50000	50000	45000	35000	30000

Table C2: Number of generated samples(other than those with 10,000) for $L = 16$

Temperature	0.05	0.115	0.179	0.244	0.308	0.373
Number of samples	70000	65000	60000	55000	50000	45000
Temperature	0.437	1.082	1.147	1.211	1.276	1.340
Number of samples	40000	70000	70000	65000	55000	50000

Table C3: Number of generated samples(other than those with 10,000) for L = 32

Temperature	0.05	0.115	0.179	0.244	0.308	0.373
Number of samples	100000	90000	85000	80000	70000	65000
Temperature	0.437	1.082	1.147	1.211	1.276	1.340
Number of samples	60000	100000	100000	90000	85000	75000

Table C4: Number of generated samples(other than those with 10,000) for L = 64

Temperature	0.05	0.115	0.179	0.244	0.308	0.373
Number of samples	120000	110000	105000	100000	90000	85000
Temperature	0.437	1.082	1.147	1.211	1.276	1.340
Number of samples	80000	120000	120000	110000	105000	95000

Table C5: Number of generated samples(other than those with 10,000) for L = 128

Appendix D Results of Experiments for PBMG-XY

L	EMD		% OL	
	Mean	Std	Mean	Std
8	0.025	0.079	80.614	11.009
16	0.022	0.050	82.304	11.767
32	0.034	0.083	76.684	23.320
64	0.052	0.138	69.366	27.801
128	0.029	0.053	68.973	26.781

Table D6: Metrics for Mean Magnetization

L	EMD		% OL	
	Mean	Std	Mean	Std
8	0.012	0.030	91.637	7.967
16	0.026	0.084	89.294	12.054
32	0.219	0.834	88.478	17.902
64	0.036	0.099	90.951	7.573
128	1.037	4.410	92.128	7.729

Table D7: Metrics for Mean Vorticity

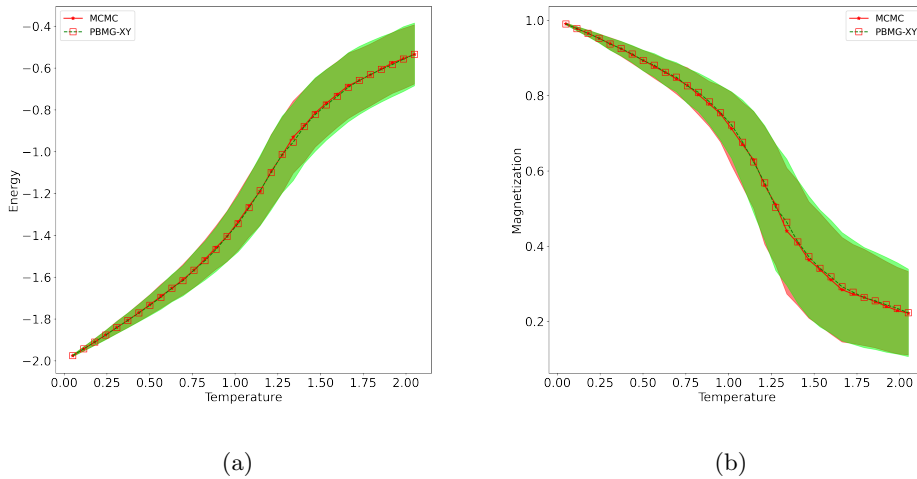
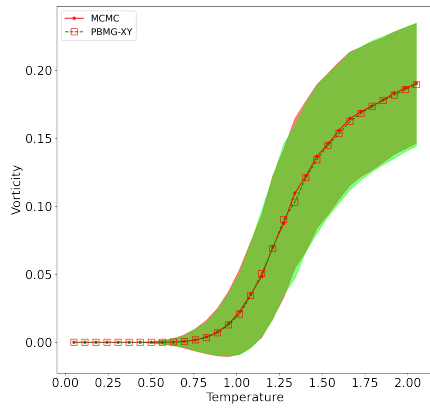
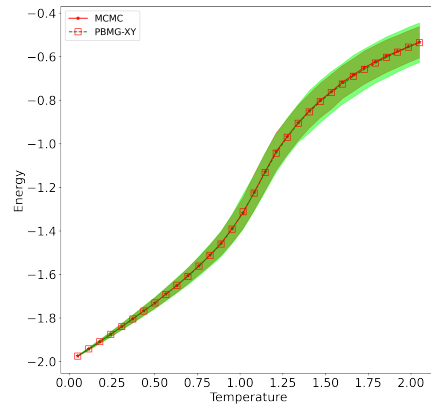


Fig. D1: a) Mean Energy and b) Mean Magnetization plots superimposed for L=8.

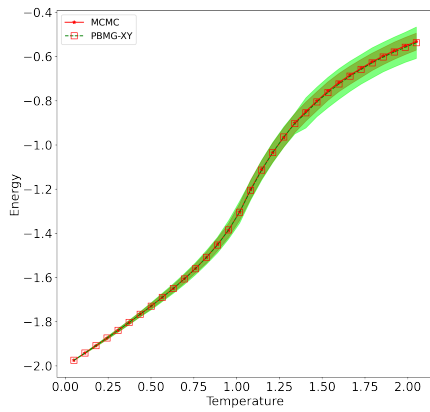


(a)

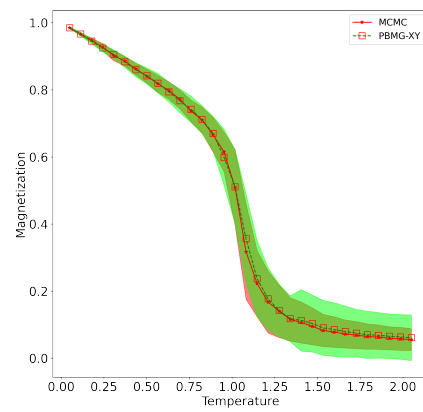


(b)

Fig. D2: a) Mean Vorticity and b) Mean Energy plots superimposed for $L=8$ and $L=16$ respectively.

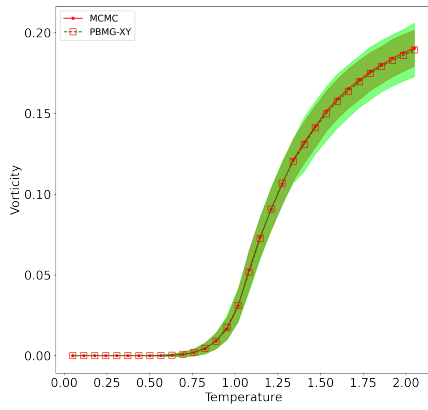


(a)

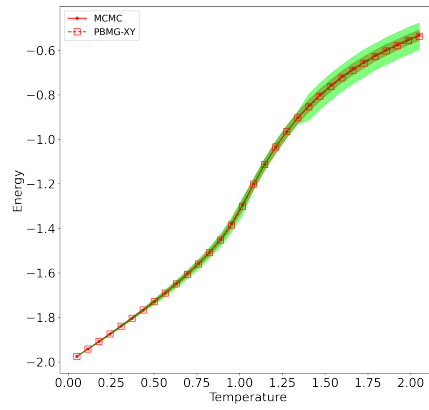


(b)

Fig. D3: a) Mean Energy and b) Mean Magnetization plots superimposed for $L=32$.

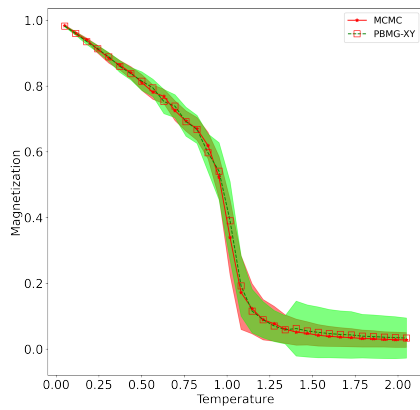


(a)

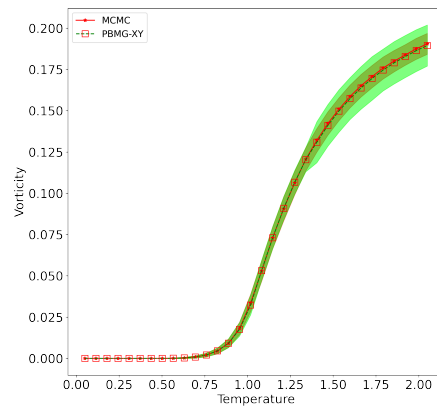


(b)

Fig. D4: a) Mean Vorticity and b) Mean Energy plots superimposed for $L=32$ and $L=64$ respectively.



(a)



(b)

Fig. D5: a) Mean Magnetization and b) Mean Vorticity plots superimposed for $L=64$.

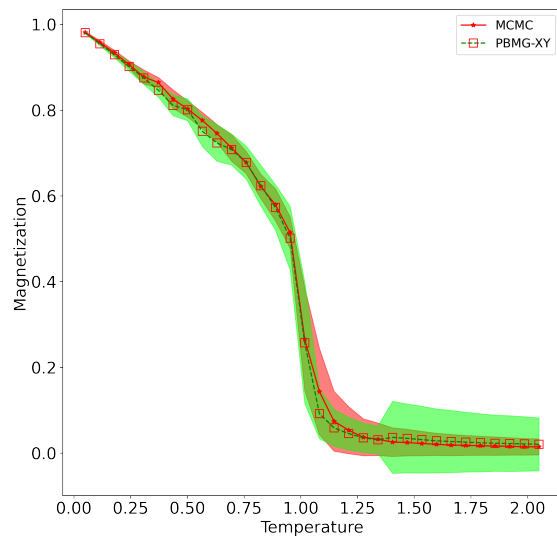


Fig. D6: Mean Magnetization plots superimposed for $L=128$